applied sciences

MDPI

Article

A Numerical Investigation of the Thermal Performance of a Gabion Building Envelope in Cold Regions with a Mountainous Climate

Fang Liu [1], Yafei Li [1], Yushi Wang [2], Qunli Zhang [1,2,*], Wei Gao [1,3] and Ying Cao [3]

[1] Beijing Key Lab of Heating, Gas Supply, Ventilating and Air Conditioning Engineering, Beijing University of Civil Engineering and Architecture, Beijing 100044, China; liufang@bucea.edu.cn (F.L.)
[2] Center Collaborative Innovation Center of Energy Conservation & Emission Reduction and Sustainable Urban-Rural Development in Beijing, Beijing 100044, China; 2108140420005@stu.bucea.edu.cn
[3] China Architecture Design & Research Group, China National Engineering Research Center for Human Settlements, Beijing 100048, China
* Correspondence: zhangqunli@bucea.edu.cn

Abstract: Applying rock-filled gabion to buildings in cold regions with mountainous climates has multiple potentials, such as utilizing rock resources, improving building sustainability and saving building energy. Therefore, it is necessary to analyze the thermal performance of gabion buildings. Based on the CFD method, this paper establishes a numerical model of buildings with gabion enclosure structures, analyzes the influence of the gabion structure on the external convective heat transfer coefficient (CHTC), wind pressure, air infiltration, room temperature and building load, and further uses the building energy consumption simulation method to analyze the heat load of gabion buildings. The results showed that the adverse impact of climate on the building thermal performance is significantly diminished by the gabion. Under different weather conditions, the CHTC, the maximum wind pressure difference on the exterior surface, and the air infiltration rate are reduced by different rates. Further, the room base temperature increases throughout the heating season, and the maximum heat load and the cumulative heat load of the building are, respectively, reduced by 10.6% and 24.8%. This work revealed that the gabion is an eco-friendly and adaptive measure to improve thermal performance and indoor thermal comfort.

Keywords: gabion; mountainous climate; cold region; building envelope thermal performance; numerical simulation

Citation: Liu, F.; Li, Y.; Wang, Y.; Zhang, Q.; Gao, W.; Cao, Y. A Numerical Investigation of the Thermal Performance of a Gabion Building Envelope in Cold Regions with a Mountainous Climate. *Appl. Sci.* **2023**, *13*, 8809. https://doi.org/10.3390/app13158809

Academic Editor: Agus Pulung Sasmito

Received: 6 July 2023
Revised: 25 July 2023
Accepted: 28 July 2023
Published: 30 July 2023

1. Introduction

The building sector accounts for about 40% of the global energy consumption [1]. In China, the energy consumption in buildings accounted for 27.6% of total national energy consumption in 1999, increasing to 45.5% by 2020 [2,3]. This proportion means there is high energy-saving potential in buildings. A building envelope has the function of regulating and controlling the use of energy because it is on the boundary between indoor and outdoor environments; therefore, the improvement of its performance has attracted attention all over the world [4–6]. Related research has mainly focused on the following problems: (1) the development of building materials with excellent thermal performance; (2) the integration of the building envelope with renewable energy; and (3) numerical and experimental investigations into the thermal performance of building envelopes. Moreover, with rapid economic growth, the strategies adapted to regional climate and environment are more cost-effective for improving building performance in reducing energy consumption and reducing the associated CO_2 emissions [7–9].

Many research efforts took more into account climate characteristics when improving the thermal performance of building envelopes and verified their effectiveness in reducing energy consumption [10–12]. And the heating and cooling requirements of passive

buildings varied considerably in different climate regions [13]. Rock is the most convenient and abundant material in mountainous regions. In terms of thermal comfort, traditional single-layer rock envelope cannot meet human demand with HVAC system; with regard to safety, it is prone to collapse owing to non-uniformity. Due to rock's good ecological expression and architectural value, gabion architecture was first introduced by designers to further overcome shortcoming of traditional rock envelope [14].

Kairl et al. [15] compared the thermal performance of traditional buildings and gabion buildings through dynamic simulation. They found that gabion buildings had better thermal performance in temperate climates. However, the mountainous climate is a special local microclimate with poor weather, characterized by high variations in wind speed and temperature [16]. Mariani et al. [14] analyzed case studies of massive single-layer stone masonry building solutions and found that, in terms of thermal energy performance, these solutions are appropriate for historical centers, maintaining urban cultural identity while ensuring energy efficiency and user comfort. Quan et al. [17] compared the thermal performance of rubble, rammed earth, gabion, and traditional cement walls. The results indicated that gabions demonstrated the best thermal delay performance, with the most stable wall heat transfer, and the least fluctuation in inner wall temperature due to changes in outer wall temperature. Interestingly, gabion buildings were also found in the Yanqing area with typical mountainous climate in Beijing, and they also achieved excellent comfort in winter. These buildings have broken people's common sense. Thus, it is valuable to quantify the adaptivity and validness of a gabion envelope for low-energy and low-carbon buildings in the mountainous region.

Thermal performance is the main approach to evaluating building envelopes. As one of the important thermal properties of the building envelope, the exterior convective heat transfer coefficient (CHTC) is a vital indicator in evaluating the thermal performance of building envelopes [18]. Besides experiments, the numerical approach is used to simulate the heat transfer between the building facades and external environments and analyze the effects of different parameters on CHTC by obtaining detailed velocity and temperature field information [19–21]. Iousef et al. [22] applied multiple exterior CHTC models to simulate the energy demand of buildings with different geometry in EnergyPlus software. The results indicated that considering building geometry, CHTC models can accurately predict building energy demand, especially for high-rise buildings. Kahsay et al. [23] carried out CFD and heat transfer simulations for high-rise buildings with and without the facade appurtenances, and concluded that local-CHTC variation and the effect of wind directions are nonnegligible for buildings with facade appurtenances.

Additionally, attention should be paid to air infiltration caused by the airtightness of building envelopes during the improvement of thermal comfort and energy efficiency under different climates [24,25]. For instance, the predicted annual energy-saving potential is 3–36% for office buildings in different climates zones of the U.S. [26], and 2.43–16.44 kWh/m^2 for dwellings in the Mediterranean climate area of Spain [27]. Since wind and buoyancy act simultaneously on air infiltration [28], wind pressure distribution on the exterior surface of the building should be considered in the energy efficiency of buildings in cold regions. Furthermore, room base temperature, which represents the hourly indoor air temperature without the air conditioning and heating system operating, is indispensable to assess the indoor thermal environment and the energy-saving potential of building envelopes [29–31].

The target building cluster faces weather characteristics distinctly different from those of the plains, which are located at the Haituo Mountains of the Yanqing region in Beijing, China. Considering features like low temperature, high wind speed and uneven precipitation distribution, gabions may affect the thermal performance of the building by changing the wind speed on the exterior wall surface. Traditional studies mainly analyze the effect of gabions on building reinforcement and force [32–34], but there are few models for building thermal processes and performance analyses. Therefore, this paper establishes a building thermal process analysis model based on the gabion structure, focusing on the analysis of the heat transfer and airflow between a simulated gabion building and the

external environment. The model was validated based on experiment results from the literature. Then, the influences on the CHTC, wind pressure, and air infiltration were analyzed. The room base temperature and the building heating load were simulated in DeST software by inputting CFD simulation results. This study could guide the thermal design of the new buildings and the energy-saving retrofits of existing buildings in cold regions with similar climates.

2. Physical Model

The gabion used in the buildings is placed outside all exterior walls, as shown in Figure 1a. A building in the south of the building group was selected as the research object. As with the others, it is surrounded by a gabion with the same height as the building. Figure 1b shows the building's plan. The distance between gabions and the exterior walls and the thickness of the gabion were, respectively, set to 100 mm and 200 mm, reflecting the dimensions and locations while avoiding errors such as negative volume grids and poor grid quality in the later meshing stage. The structure of the gabion building envelope is as illustrated in Figure 2. The combination of gabion envelopes and reinforced concrete load-bearing structures improves the level of safety. Based on the principle of controlled variables, we consider that the main difference between the ordinary external building envelope and the gabion building envelope is the absence or presence of the gabion structure. The exterior wall is structurally identical and has the same physical parameters. The relevant thermo-physical properties of materials used in the envelope are listed in Table 1. After preliminary field research of the Yanqing region, a physical model of this building group was established in Fluent software according to the surveyed terrain. The buildings were simplified to corresponding size blocks, neglecting the support elements within the building in this physical model. As shown in Figure 3, the exterior surfaces of the analyzed building were numbered for the convenience of analysis.

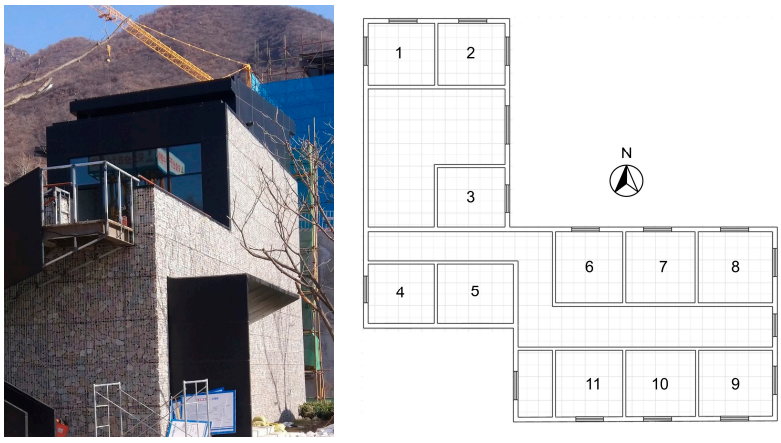

(**a**) (**b**)

Figure 1. (**a**) Gabion used in the buildings; (**b**) the research building's layout.

Table 1. Relevant thermo-physical properties of materials.

Material	Thermo-Physical Properties		
	Conductivity (W/(mK))	Specific Heat (J/(kg·K))	Density (kg/m^3)
Anti-cracking mortar [35]	0.93	1050	1800
Polystyrene sheet [35]	0.042	1380	30
Reinforced concrete [36]	1.74	920	2500
Lime gypsum mortar [35]	0.76	1050	1500
Stone [35]	1.04	1000	2000

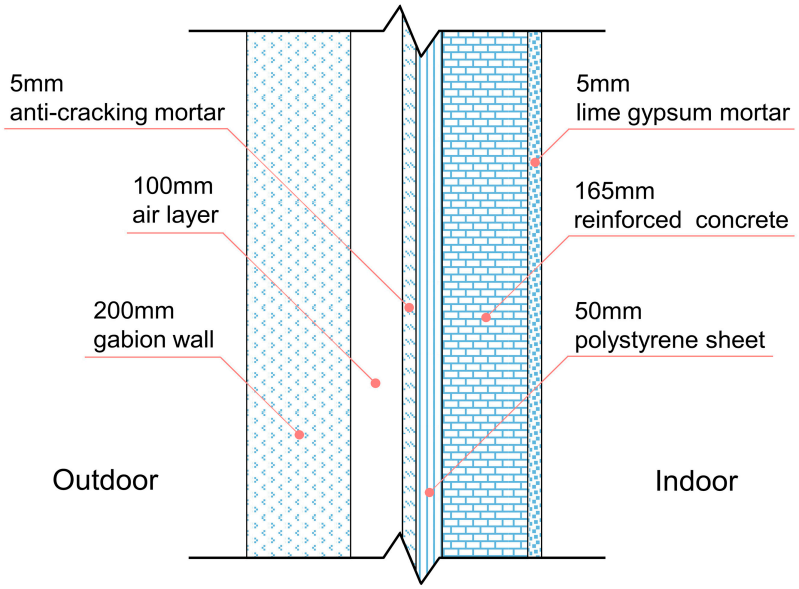

Figure 2. Schematic of the gabion building envelope.

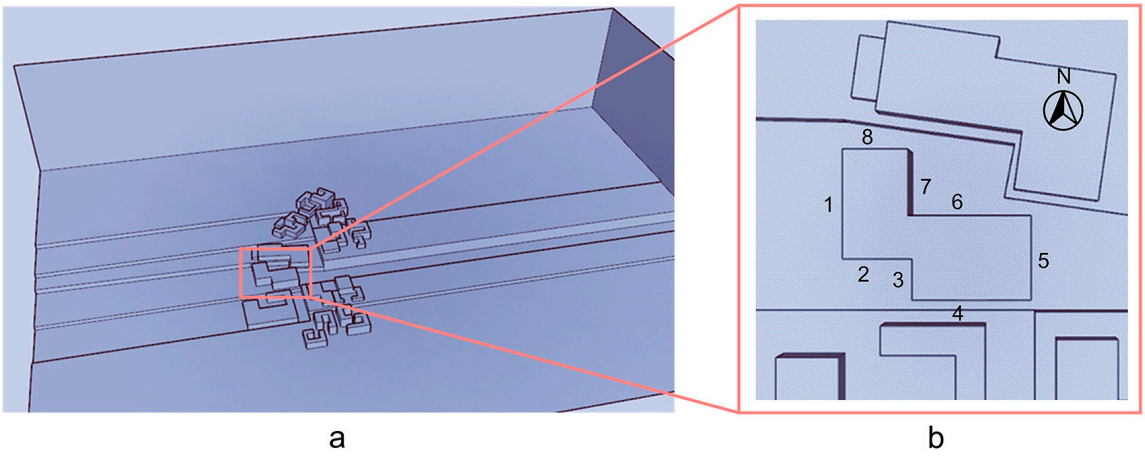

Figure 3. (**a**) Building physical model; (**b**) exterior surface numbers of the analyzed building.

3. Mathematical Model

3.1. Computational Domain, Grid and Boundary Condition

The computational domain (Figure 4) was built to simulate the external environment, with a size of 1425 m (length) × 945 m (width) × 302 m (height). The dimensions were defined based on the recommendation relationship [37] between the height of the tallest building and the dimensions. The inlet boundary wall is set at 6H from the exterior building surface, with the outlet boundary 15H downstream of the building, to allow for full development of the wake-flow. The distances between the lateral boundaries and the building are 5H when the height of the computational domain is 5H.

The areas adjacent to the exterior building surfaces and the gabions are key areas that are finely meshed using an unstructured mesh. The far-field area is sparsely meshed, whereas the closer one is to the gabions, the finer the mesh is divided. Moreover, the fineness of the mesh in the near-wall region matches the near-wall turbulent flow model.

The boundary conditions of the computational domain are given in detail in Table 2. To simulate the variation in wind speed with height and underlying surface situation in

the external environment, an exponential profile is chosen as the incoming wind velocity profile for the inlet of the domain and the equation is shown as follows:

$$v = v_{ref}\left(\frac{z}{z_{ref}}\right)^{0.14} \quad (1)$$

where, v and v_{ref} are the velocity for the inlet and reference point, respectively. z and z_{ref} are the vertical height for inlet and reference point, respectively. Moreover, the standard wall function is used for the near-wall areas. The temperature of the exterior building surface under simulation conditions can be calculated based on the basic principles of heat transfer.

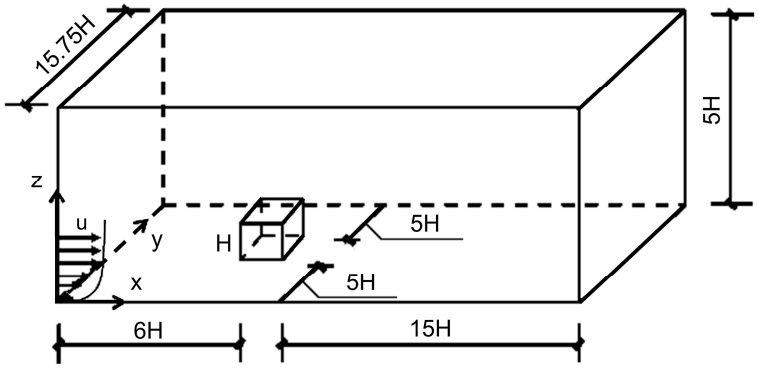

Figure 4. Computational domain (H: height of the tallest building).

Table 2. Boundary conditions for simulation.

Item	Boundary Type	Boundary Condition Setting
Inlet	Velocity inlet	Velocity: 3 m/s, 5 m/s and 10 m/s [38–40] Temperature: −10 °C, −20 °C, −27 °C [38–40]
Outlet	Pressure outlet	
Exterior building surface/gabion	Wall	Temperature: Data from calculation Non-slip
Lateral and top side of the domain	Symmetry	
Ground surface	Wall	Adiabatic

3.2. Governing Equations

To emphasize the physical essence and facilitate the numerical calculation, we made the following assumptions:

1. The temperature of the exterior building surface is uniformly distributed;
2. Indoor heat disturbance was ignored;
3. The air is a Newton fluid that satisfies the boussinesq assumption;
4. The thermal contact resistance between different layer of the exterior wall were ignored;
5. The change in thermal conductivity with temperature was ignored, and the thermal conductivity was constant.

The Reynolds-averaged Navier–Stokes equations are used to describe the turbulent flow because they can excellently express the statistical average of the physical quantities and other statistical randomness in turbulence. With good convergence and a low memory footprint, the Standard k-ε model can be used in the exterior flow with complex geometries as well as non-slip wall flow, which uses wall functions to analyze fluid velocities in the viscous sublayer near the wall. Therefore, the Standard k-ε model was used to solve the Reynolds stress term in this study. The governing equations are given in Table 3.

Table 3. The governing equations.

Type	Mathematical Model	Definition
Continuity equation	$\frac{\partial \overline{V}_i}{\partial x_i} = 0$	$\overline{V}_i$ averaged velocity vector $\overline{p}$ averaged pressure $\overline{T}$ averaged temperature ρ air density c_p air specific heat λ air thermal conductivity μ air dynamic viscosity $-\rho V_i' V_j'$ Reynolds stress term, solved by the standard k-ε model σ_k turbulent Prandtl numbers for k σ_ε turbulent Prandtl numbers for ε c_1 equals to 1.44 c_2 equals to 1.92 μ_t the turbulent viscosity, defined as $\rho C_\mu \frac{k^2}{\varepsilon}$ C_μ equals to 0.09
Momentum equation	$\frac{\partial(\rho \overline{V}_i)}{\partial t} + \frac{\partial(\rho \overline{V}_i \overline{V}_j)}{\partial x_j} = -\frac{\partial \overline{p}}{\partial x_i} + \frac{\partial}{\partial x_j}\left(\mu \frac{\partial \overline{V}_i}{\partial x_j} - \rho V_i' V_j'\right)$	
Energy equation	$\frac{\partial(\rho c_p \overline{T})}{\partial t} + \frac{\partial(\rho c_p \overline{T V}_j)}{\partial x_j} = \frac{\partial}{\partial x_j}\left(\lambda \frac{\partial \overline{T}_i}{\partial x_j} - \rho c_p T' V_j'\right)$	
The standard k-ε model	$\frac{\partial(\rho V_i k)}{\partial x_i} = \frac{\partial}{\partial x_i}\left[\left(\mu + \frac{\mu_t}{\sigma_k}\right)\frac{\partial k}{\partial x_i}\right] + \mu_t\left(\frac{\partial V_j}{\partial x_i} + \frac{\partial V_i}{\partial x_j}\right)\frac{\partial V_j}{\partial x_i} - \rho\varepsilon$ $\frac{\partial(\rho V_i \varepsilon)}{\partial x_i} = \frac{\partial}{\partial x_i}\left[\left(\mu + \frac{\mu_t}{\sigma_\varepsilon}\right)\frac{\partial \varepsilon}{\partial x_i}\right] + \frac{c_1 \varepsilon}{k}\mu_t\left(\frac{\partial V_j}{\partial x_i} + \frac{\partial V_i}{\partial x_j}\right)\frac{\partial V_j}{\partial x_i} - c_2\frac{\rho\varepsilon^2}{k}$	

3.3. Working Conditions

This research aims to study the thermal performance of the gabion building envelope and verify its high-performance potential for saving energy in cold regions with a mountainous climate. As the heat transfer process of the building envelope is necessarily affected by the weather, the complete meteorological data is indispensable to accurate simulation results. The Haituo Mountain, with complex geological conditions, has a typical mountainous climate, and is located in Beijing (a representative city in the cold region of China). The winter is characterized by high wind, uneven precipitation, and large diurnal temperature range. The weather data for the building was derived from the literature [38–40] involving the meteorological parameters of the Haituo Mountain. The Haituo Mountain shows different minimum temperatures and maximum wind speeds during cold waves, and the dominant wind direction in winter is west. Given all these considerations, the three most typical types of weather in winter are selected, including the normal, snowy cold wave, and windy cold wave. The details of the weather corresponding to simulation conditions are shown in Table 4.

Table 4. Simulation conditions.

Item Number	Weather	Wind Direction	Air Temperature (°C)	Wind Speed (m/s)	Air Density (kg/m^3)	Air Thermal Conductivity $\times 10^{-2}$/(W/(m·K))	Air Specific Heat (kJ/(kg·K))	Air Kinematic Viscosity $\times 10^{-5}$/(m^2/s)
I	Normal	West	−10	3	1.342	2.360	1.0090	1.243
II	Snowy cold wave	West	−20	5	1.395	2.279	1.0090	1.161
III	Windy cold wave	West	−27	10	1.436	2.255	1.0118	1.104

3.4. Grid Independence Verification

To exclude the influence of the number of mesh cells in the computational domain on the simulation results, a grid independence verification was performed with four different grid sizes, as shown in Table 5. The result of the model with 3,135,433 cells was used as a reference. As the number of grids increased, the relative error of the CHTC on the exterior surface varied insignificantly. The effect of the grid number on the simulation results could be neglected with less than 7.69% difference. Considering the computing

speed and the accuracy of the results, it is reasonable to create 3,135,433 cells for discretizing computational domain in the numerical simulation.

Table 5. Grid independence verification.

Number of Cells	The CHTC Value (W/(m^2·K))	Relative Error (%)
2,894,941	7.91	4.91
3,135,433	7.54	-
5,383,569	7.16	5.04
8,760,834	8.12	7.69

3.5. Model Validation

The numerical model was validated by comparing the simulation results of the No. 4 exterior surface without gabion structure with the experiment results [41] under three wind speed levels: 1.5 m/s, 2.0 m/s and 4.5 m/s. The CHTCs of the simulation result, the experimental data and the corresponding fitted curves are shown in Figure 5. The maximum difference between the simulation results and the experimental data is 0.968 W/(m^2·K) (7.10%). Therefore, it can be concluded that the CHTCs from the simulation results agree well with the experimental data, demonstrating that this numerical model could predict the heat transfer between exterior surface and external environment well.

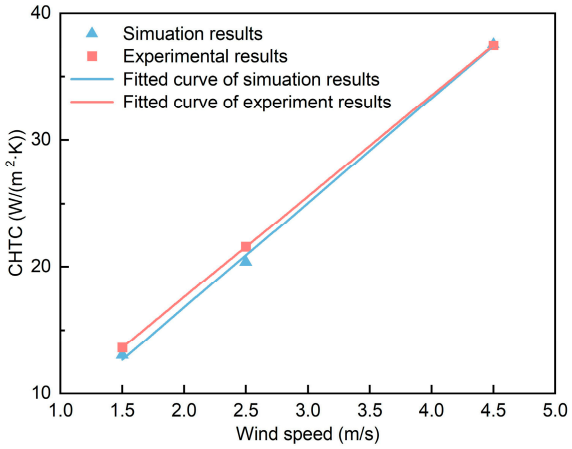

Figure 5. The exterior CHTC in the simulation results and the experiment results [38].

4. Results and Discussion

4.1. Effect of Gabion on the Exterior CHTC

The calculated CHTC values on the exterior surfaces of a building with or without gabion under different weather conditions (Figure 6) show the effect of this structure surrounding the exterior wall on the exterior CHTC. Generally, the gabion could significantly reduce the exterior CHTC under all simulation conditions, even in cold wave weather. The averaged CHTC value is reduced by 7.660 W/(m^2·K) (69%), 11.373 W/(m^2·K) (67%), and 18.530 W/(m^2·K) (63%) for three simulation conditions. As shown in Figure 6, the CHTC values on the different exterior surfaces are more even and fluctuate less when the exterior wall is surrounded by gabion. It is evident that the gabion can significantly weaken the effect of severe weather on the exterior CHTC.

For the building without gabions, the maximum is found at the No. 3 exterior surface when higher values of CHTC are observed at the No. 2, 3, and 4 external surfaces of the building under all simulation conditions. However, with gabion, CHTC values of the above three exterior surfaces are reduced and close to those of other exterior surfaces. Further, the CHTC value of exterior surface No. 3 is reduced from 47.853 W/(m^2·K) to 7.925 W/(m^2·K) with a reduction of 83.4% during the windy cold wave weather of condition III. The flow structure is considerably influenced by the buildings' geometry, which affects the

distribution of CHTC. Unlike other exterior surfaces, the No. 2 and 4 exterior surfaces are parallel to the direction of the incoming flow and not sheltered by other buildings or the building itself. As a result, higher wind speeds are observed near the surfaces. The No. 3 external surface has the highest surface velocity for the building without gabions due to its location, as illustrated in Figure 7. The vortices flowing from No. 3 exterior surface to No. 2 exterior surface in the corner area of the building, which decreases the air residence time, results in the highest velocity of No. 3 exterior surface. Moreover, since the wind speed is higher, the CHTCs are larger. When the gabion is set, the near-wall velocities at the No. 2, 3, and 4 exterior surfaces are effectively decreased, and thus so are the corresponding CHTCs. The reduction in CHTC might be explained by the fact that gabion can effectively reduce the surface velocity of the exterior building surface parallel to the direction of the incoming flow, demonstrating that it diminishes the effect of flow structure on the exterior CHTC.

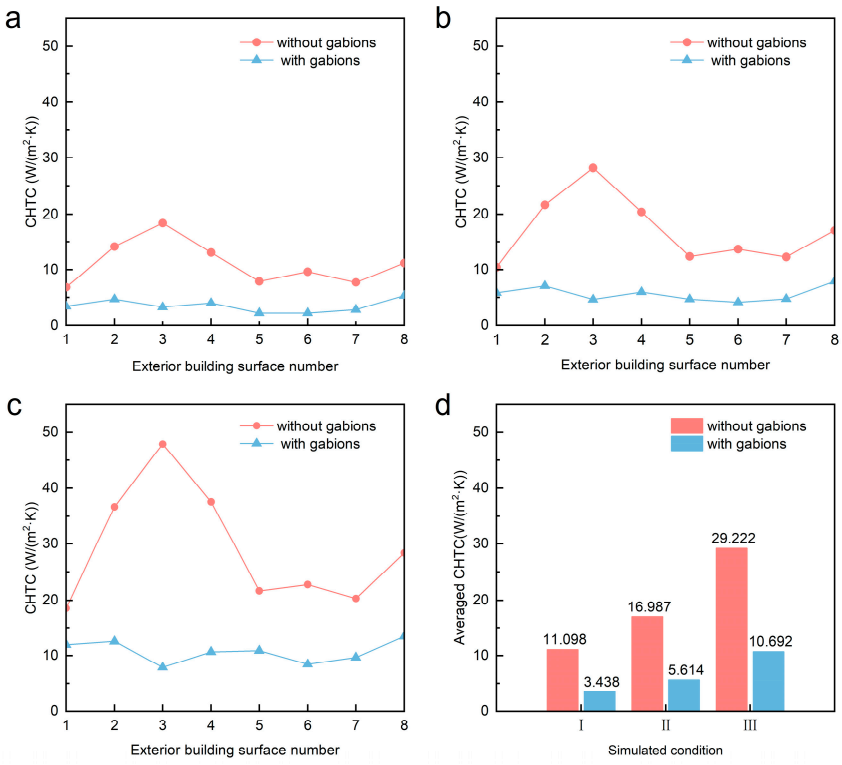

Figure 6. CHTC on each exterior building surface and averaged CHTC under three simulation conditions: (**a**) condition I; (**b**) condition II; (**c**) condition III; (**d**) averaged CHTC.

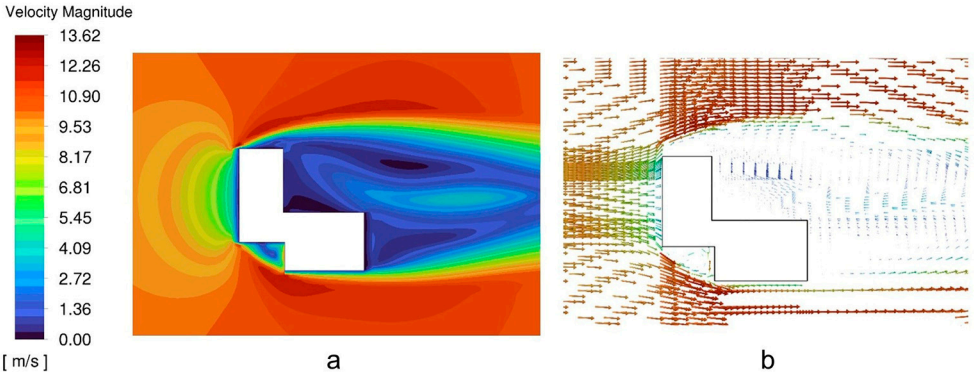

Figure 7. Velocity magnitude contour and vector (at 10 m ref height for the building without gabions under condition III): (**a**) contour; (**b**) vector.

4.2. Effect of Gabion on Wind Pressure and Air Infiltration

The wind pressures on the exterior surfaces of buildings with/without the gabion in three simulation conditions are shown in Figure 8. It can be seen that the wind pressure distribution on exterior surfaces is significantly altered by setting the gabion under different weather, which is more pronounced in cold wave weather. While the wind pressure distribution of the building without gabion has both positive and negative pressure zones, that of the building with gabion only has the negative pressure zone; the wind pressures of the No. 1 and 3 exterior surfaces change from positive to negative. The higher variation in wind pressure shows that the No. 1 and 3 exterior surfaces are more sensitive to the gabion. However, the wind pressures of the others that are not windward are almost unaffected after setting the gabion. This might be attributed to the fact that the gabion weakens this effect on wind pressure when the No. 1 and 3 exterior surfaces are considerably affected by the incoming airflow as windward sides.

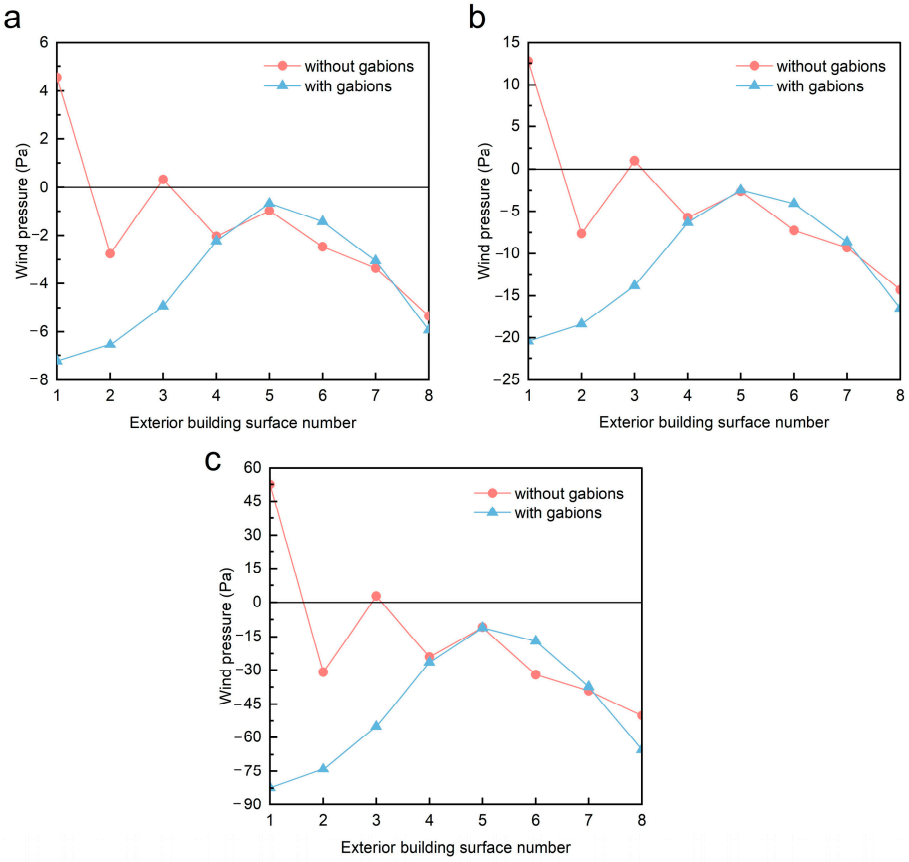

Figure 8. Wind pressure on exterior building surface under three simulation conditions: (**a**) condition I; (**b**) condition II; (**c**) condition III.

The gaps in windows and doors are the main pathway for cold air to enter the building [28]. For multi-story buildings, infiltration heat loss is mainly influenced by the amount of infiltration through external windows due to wind pressure, which is related to the position of the external windows [42]. The critical factor of the wind-driven infiltration is the indoor–outdoor wind pressure difference, increasing with the difference between the wind pressure on the windward side and that of the leeward side [43]. Under all simulation conditions, the maximum pressure difference is obtained between the No. 1 and 8 exterior surfaces for the building without the gabion, while between the No. 1 and 5 exterior surfaces after using the gabion. And the maximum pressure difference is, respectively, reduced by 4.283 Pa (43.5%), 9.186 Pa (33.9%), and 31.41 Pa (30.6%). Therefore, based on simplified theoretical equations [44], the wind-driven air infiltration rates of the building with gabions, respectively, are all reduced considerably in conditions I, II, and III.

Due to its impact on the wind pressure distribution of the exterior building surface, the gabion can reduce the air infiltration rate to decrease the building heat load caused by cold air infiltration. Apart from taking proactive measures to increase the airtightness of the envelope, installing the gabion is also an effective way to mitigate the effect of the environment and air infiltration on building energy consumption in a harsh outdoor environment.

4.3. Impact of Gabion on Room Base Temperature

The room base temperature of a building is an inherent parameter that reflects the comprehensive regulation of the building envelope under the external environment. To explore the effect of the gabion on the room base temperature, a simulation was carried out by inputting the exterior CHTCs and the weather information of condition I in the DeST software. The thermal characteristics of the envelope are listed in Table 6. The air exchange rate was set as 0.5 ACH. The heating set-point was 20 °C and there was no heat exchange between rooms because of the same indoor temperature. A 3.5 W/m^2 lighting system was equipped in the room. Moreover, a residential building occupancy of four people with an activity schedule of 18 p.m. to 8 a.m. on workdays is considered. The simulation period was from 15 November to 15 March (i.e., normal heating season) in a typical year. The numerical results are displayed in Figure 9.

Table 6. Thermal characteristics of envelope.

Envelope	Thermal Transmittance (W/(m^2·K))
Normal exterior wall	0.177
Gabion building envelope	0.171
Roof	0.393
Window	2.5

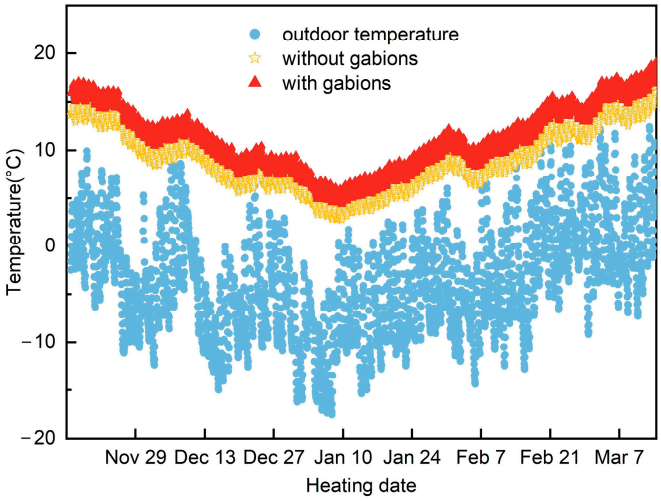

Figure 9. Impact of the gabion on room base temperature during heating season.

The gabion is effective in increasing room base temperature for the building in cold regions with a mountainous climate. It is observed that the room base temperature of a building with gabions is higher than that of a traditional building during the heating season, while its daily fluctuation range is nearly unchanged. The average room base temperature for the building with and without the gabion structure is 11.21 °C and 9.18 °C; the rate of increase is 22%. This increase in the room base temperature indicates an improved thermal insulation performance of the building envelope, which could reduce the energy

consumption for building heating and enhance the adaptive capacity of a building to outdoor environments.

4.4. Impact of Gabion on Building Load

Building load is a crucial indicator to evaluate the thermos-physical performance of a building. Using the gabion has a pronounced effect on the room base temperature, which inevitably changes the building load. The building heat load of condition I was selected as the research subject. The discussed heating period was the same as in Section 4.3, and DeST software was applied to simulate the effect of the gabion building envelope on the building heat load. The maximum heat load and cumulative heat load of the building with and without the gabion are presented in Figure 10. In comparison to the traditional building, the use of gabions leads to a maximum heat load saving of 83.38 kW (10.7%) and a cumulative heat load saving of 80,970.46 kWh (24.8%) during the heating season. Therefore, adding gabions results in good performance for reducing heating energy consumption of buildings in cold regions.

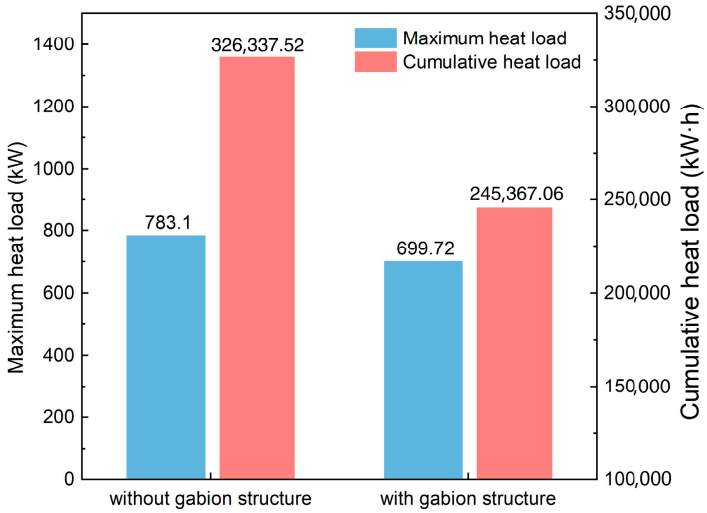

Figure 10. Impact of the gabion on maximum heat load and cumulative heat load for the heating season.

5. Conclusions

During the buildings' design stage, weakening the impact of the mountain environment on the thermal performance of buildings is an effective strategy for achieving energy efficiency in cold regions with a mountainous climate. In this study, a numerical model was developed to evaluate the thermal performance of a gabion building envelope under three weather conditions, and it was compared to the traditional building envelope. The effect on the convective heat transfer coefficient (CHTC), the wind pressure and the air infiltration were investigated by using CFD and heat transfer simulations. Then, DesT simulations were conducted by using the CHTC results to comparatively illustrate the impact on room base temperature and building load. It is fair to say that the gabion can enhance a building's thermal performance in mountainous climate regions, resulting in the improvement of building energy efficiency and thermal comfort. The main conclusions can be drawn as follows:

1. Regardless of the weather condition, gabion significantly reduces the CHTC on the exterior building surface by effectively reducing the wind speed on the external building surface, even that of a surface parallel to the incoming flow direction. These leads to a 69% decrease in the average CHTC value for the building under condition I, 67% under condition II, and 63% under condition III;
2. The gabion can obviously change the wind pressure distribution on the exterior building surface, reduce the maximum wind pressure difference on external surfaces of the building envelope, and effectively weaken the impact of air infiltration

on the building's energy consumption. Compared to a building without gabions, the air infiltration rate of a building with gabions is also greatly reduced under three conditions;

3. A gabion located on the outside of the exterior wall can improve the room base temperature throughout the heating season, and the average room base temperature is 2.02 °C higher than that of a building without gabions. Therefore, a gabion can have a significant impact on saving energy for building heating and enhancing the adaptability to the unfriendly external environment;
4. The gabion structure has a non-negligible influence on the heating load while lowering the maximum heat load (up to 10.7%) and the cumulative heat load (up to 24.8%) during the heating season.

The thermal performance of gabion buildings in a mountainous climate is examined in this paper, and a feasible analysis model and research method are provided. In the future, the thermal performance of gabion buildings under other climatic conditions could be further analyzed. Additionally, it becomes necessary to further construct an experimental system and employ experimental methods for conducting related performance analysis.

Author Contributions: Conceptualization, F.L. and Q.Z.; methodology, Y.L.; software, W.G.; validation, F.L., Y.L. and Q.Z.; formal analysis, Y.W.; investigation, F.L.; resources, Q.Z.; data curation, Y.L.; writing—original draft preparation, F.L.; writing—review and editing, Y.L.; visualization, Y.W.; supervision, Q.Z.; project administration, Y.C. All authors have read and agreed to the published version of the manuscript.

Funding: This research received no external funding.

Institutional Review Board Statement: Not applicable.

Informed Consent Statement: Not applicable.

Data Availability Statement: The data presented in this study are shown in the paper.

Conflicts of Interest: The authors declare no conflict of interest.

References

1. Xu, X.; Dessel, S.V. Evaluation of an Active Building Envelope window-system. *Build. Environ.* **2008**, *43*, 1785–1791. [CrossRef]
2. Lang, S.W. Current situation and progress of energy efficiency design standards in buildings in China. *Refrig. Air Condition Elect. Power Mach.* **2002**, *24*, 1–6.
3. China association of building energy efficiency. 2022 research report of China building energy consumptionand carbon emission. *Constru. Build.* **2023**, *2*, 57–69.
4. Wang, X.; Sun, X.; Yu, C.W.F. Building envelope with variable thermal performance: Opportunities and challenges. *Indoor Built Environ.* **2018**, *27*, 729–733. [CrossRef]
5. Wang, X.; Cheng, R.; Zeng, R.; Zhang, Y. Ideal thermal physical properties of building wall in an active room. *Indoor Built Environ.* **2014**, *23*, 839–853. [CrossRef]
6. Far, C.; Far, H. Improving energy efficiency of existing residential buildings using effective thermal retrofit of building envelope. *Indoor Built Environ.* **2019**, *28*, 744–760. [CrossRef]
7. Xu, J.; Lu, Z.L.; Gao, W.J.; Yang, M.S.; Su, M.L. The comparative study on the climate adaptability based on indoor physical environment of traditional dwelling in QinBa mountainous areas, China. *Energy Build.* **2019**, *197*, 140–155.
8. Chantrelle, P.F.; Lahmidi, H.; Keilholz, W.; Mankibi, M.E.; Michel, P. Development of a multicriteria tool for optimizing the renovation of building. *Appl. Energy* **2011**, *88*, 1386–1394. [CrossRef]
9. 9. Shohan, AAA. Thermal Comfort and Energy Demand of Small and Large Mosque Buildings in Saudi Arabia. Ph.D. Thesis, University of Nottingham, Nottingham, UK, 2015.
10. Philokyprou, M.; Michael, A.; Thravalou, S.; Ioannou, I. Thermal performance assessment of vernacular residential semi-open spaces in Mediterranean climate. *Indoor Built Environ.* **2018**, *27*, 1050–1068. [CrossRef]
11. Alwetaishi, M.; Taki, A. Investigation into energy performance of a school building in a hot climate: Optimum of window-to-wall ratio. *Indoor Built Environ.* **2020**, *29*, 24–39. [CrossRef]
12. Rubio-Bellido, C.; Pulido-Arcas, J.A.; Cabeza-Lainez, J.M. Understanding climatic traditions: A quantitative and qualitative analysis of historic dwellings of Cadiz. *Indoor Built Environ.* **2018**, *27*, 665–681. [CrossRef]
13. Duan, M.F.; Sun, H.L.; Wu, Y.F.; Wu, X.Y.; Lin, B.R. Climate adaptive thermal characteristics of envelope of residential passive house in China. *J. Cent. South Univ.* **2022**, *29*, 2317–2329. [CrossRef]

14. Mariani, S.; Rosso, F.; Ferrero, M. Building in Historical Areas: Identity Values and Energy Performance of Innovative Massive Stone Envelopes with Reference to Traditional Building Solutions. *Buildings* **2018**, *8*, 17. [CrossRef]
15. Lydia, K.; Veronica, S. Limitations of building performance simulation: Modelling a building with gabion walls. In Proceedings of the Conference Proceedings Building Simulation 2015, Hyderabad, India, 7–9 December 2015; Mathur, J., Garg, V., Eds.; International Building Performance Simulation Association: Shanghai, China, 2015; pp. 1700–1707.
16. Fu, B. *Mountainous Region Climate*; Science Press: Beijing, China, 1983.
17. Quan, J.; Songyue, X.; Chang, L.; Meng, J.; He, L. The Strategy of Passive Ecological Building Design Based on Guangxi's Climate Characteristics—A Case Study on the Garden Art Gallery of the 12th China (Nanning) International Garden Expo. *IOP Conf. Ser. Earth Environ. Sci.* **2021**, *768*, 012132. [CrossRef]
18. Liu, J.; Heidarinejad, M.; Gracik, S.; Srebric, J. The impact of exterior surface convective heat transfer coefficients on the building energy consumption in urban neighborhoods with different plan area densities. *Energy Build.* **2015**, *86*, 449–463. [CrossRef]
19. Emmel, M.G.; Abadie, M.O.; Mendes, N. New external convective heat transfer coefficient correlations for isolated low-rise buildings. *Energy Build.* **2007**, *39*, 335–342. [CrossRef]
20. Montazeri, H.; Blocken, B. New generalized expressions for forced convective heat transfer coefficients at building facades and roofs. *Build Environ.* **2017**, *119*, 153–168. [CrossRef]
21. Blocken, B.; Defraeye, T.; Derome, D.; Carmeliet, J. High-resolution CFD simulations for forced convective heat transfer coefficients at the façade of a low-rise building. *Build Environ.* **2009**, *44*, 2396–2412. [CrossRef]
22. Iousef, S.; Montazeri, H.; Blocken, B.; van Wesemael, P. Impact of exterior convective heat transfer coefficient models on the energy demand prediction of buildings with different geometry. *Build. Simul.* **2019**, *12*, 797–816. [CrossRef]
23. Kahsay, M.T.; Bitsuamlak, G.T.; Tariku, F. CFD simulation of external CHTC on a high-rise building with and without façade appurtenances. *Build. Environ.* **2019**, *165*, 106350. [CrossRef]
24. Emmerich, S.J.; Persily, A.K.; McDowell, T.P. Impact of infiltration on heating and cooling loads in US office buildings. In Proceedings of the 26th AIVC Conference "Ventilation in Relation to the Energy Performance of Buildings", Brussels, Belgium, 21–23 September 2005.
25. Liu, W.; Zhao, X.W.; Chen, Q.Y. A novel method for measuring air infiltration rate in buildings. *Energy Build.* **2018**, *168*, 309–318. [CrossRef]
26. *NISTIR 7238*; Investigation of the Impact of Commercial Building Envelope Airtightness on HVAC Energy Use. National Institute of Standards and Technology: Gaithersburg, MD, USA, 2005.
27. Feijó-Muñoz, J.; Pardal, C.; Echarri, V. Energy impact of the air infiltration in residential buildings in the Mediterranean area of Spain and the Canary Islands. *Energy Build.* **2019**, *188–189*, 226–238. [CrossRef]
28. Lu, Y.; Xiang, Y.; Chen, G.; Liu, J.; Wang, Y. On-site measurement and zonal simulation on winter indoor environment and air infiltration in an atrium in a severe cold region. *Energy Build.* **2020**, *223*, 110160. [CrossRef]
29. Jian, Y.; Jiang, Y. Comparison of indoor temperatures between simulation results and field measurements. *Hous. Sci.* **2002**, *23*, 3–5.
30. Da, Y.; Xie, X.; Song, F.; Jiang, Y. Building environment design simulation software DeST (1): An overview of developments and information of building simulation and DeST. *J. HVAC.* **2004**, *34*, 48–56.
31. Jian, Y.; Neng, Z. Evaluation of indoor thermal environmental, energy and daylighting performance of thermotropic windows. *Build. Environ.* **2012**, *49*, 283–290.
32. Albaji, M.; Ershadian, B.; Noori Nejad, A.; Mohammadi, E.; Ghorban Dashtaki, S. Determination of water erosion in Kowsar catchment area and evaluation of Gabion structures in its control. *Environ. Earth Sci.* **2020**, *79*, 505. [CrossRef]
33. Su, Y.C.; Choi, C.E. Effects of particle shape on the cushioning mechanics of rock-filled gabions. *Acta Geotech.* **2021**, *16*, 1043–1052. [CrossRef]
34. Lambert, S.; Bourrier, F.; Gotteland, P.; Nicot, F. An experimental investigation of the response of slender protective structures to rockfall impacts. *Can. Geotech. J.* **2020**, *57*, 1215–1231. [CrossRef]
35. Zhang, X.H.; Liu, J.X.; Zhang, H.Z. Building external wall thermal insulation construction quality safety measures analysis. *Appl. Mech. Mater.* **2013**, *253*, 646–649. [CrossRef]
36. Lu, J.; Xue, Y.; Wang, Z.; Fan, Y. Optimized mitigation of heat loss by avoiding wall-to-floor thermal bridges in reinforced concrete buildings. *J. Build. Eng.* **2020**, *30*, 101214. [CrossRef]
37. Tominaga, Y.; Mochida, A.; Yoshie, R. AIJ guidelines for practical applications of CFD to pedestrian wind environment around buildings. *J. Wind. Eng. Ind. Aerodyn.* **2008**, *96*, 1749–1761. [CrossRef]
38. Li, Z.; Yan, Z.; Tu, K. Changes in wind speed and extremes in Beijing during 1960–2008 based on homogenized observations. *Adv. Atmos. Sci.* **2011**, *28*, 408–420. [CrossRef]
39. Li, L.; Qiao, Y.; Sun, X.Q. Spatial-temporal characteristics and change trend of wind chill temperature in winter in Yanqing of Beijing. *J. Arid. Meteorol.* **2018**, *36*, 936–943.
40. Zhang, Z.G.; Cui, W.; Bai, X. Winter ground wind field characteristic in the Haituo Mountain division for the 24th Winter Olympic Games. *J. Arid. Meteorol.* **2017**, *35*, 433–438.
41. Zhang, W.W. Field Measurement and Simulation Research on the Convective Heat Transfer Coefficient of Urban Waterproof Surface. Master's Thesis, Harbin Institute of Technology, Harbin, China, 2008.
42. Lu, Y. *Practical Handbook for HVAC Design*, 2nd ed.; China Architecture & Building Press: Beijing, China, 2008.

43. Xu, Z.; Cao, G.; Zhang, M. Discussion about infiltration of contamination through doors and windows. *Build. Sci.* **2017**, *33*, 135–141.
44. Mun, J.; Lee, J.; Kim, M. Estimation of Infiltration Rate (ACH Natural) Using Blower Door Test and Simulation. *Energies* **2021**, *14*, 912. [CrossRef]